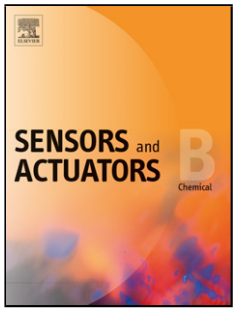

Title: Highly sensitive detection of Cr(VI) by reduced graphene oxide chemiresistor and 1,4-dithiothreitol functionalized Au nanoparticles

Author: Feng Tan Longchao Cong Xiao Jiang Yi Wang Xie Quan Jingwen Chen Ashok Mulchandani

PII: S0925-4005(17)30390-8
DOI: http://dx.doi.org/doi:10.1016/j.snb.2017.02.163
Reference: SNB 21894

To appear in: *Sensors and Actuators B*

Received date: 11-11-2016
Revised date: 5-2-2017
Accepted date: 25-2-2017

Please cite this article as: F. Tan, L. Cong, X. Jiang, Y. Wang, X. Quan, J. Chen, A. Mulchandani, Highly sensitive detection of Cr(VI) by reduced graphene oxide chemiresistor and 1,4-dithiothreitol functionalized Au nanoparticles, *Sensors and Actuators B: Chemical* (2017), http://dx.doi.org/10.1016/j.snb.2017.02.163

Highlights

- Novel AuNPs functionalized reduced graphene oxide chemiresistive sensor
- Binding of DTT-AuNPs induced by Cr(VI) ion contributed to the sensor response
- Sensitive and selective detection of Cr(VI) ion in water samples

Graphical abstrcat

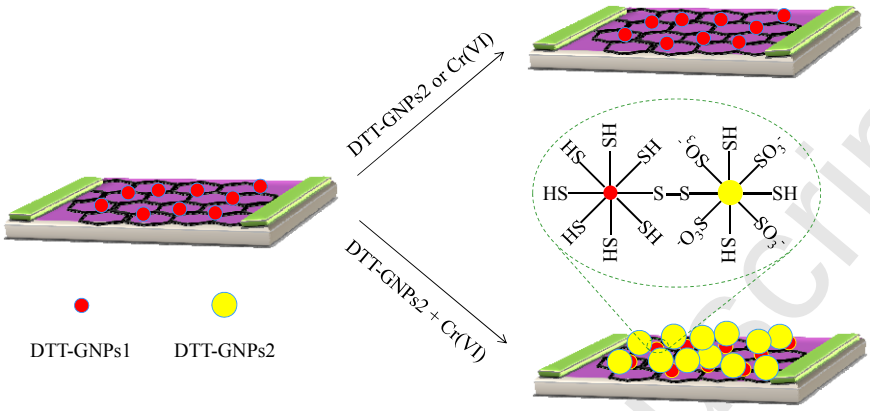

Highly sensitive detection of Cr(VI) by reduced graphene oxide chemiresistor and 1,4-dithiothreitol functionalized Au nanoparticles

Feng Tan,[a,*] Longchao Cong,[a] Xiao Jiang,[a] Yi Wang,[a] Xie Quan,[a] Jingwen Chen,[a] and Ashok Mulchandani,[b,*]

[†]*Key Laboratory of Industrial Ecology and Environmental Engineering (MOE), School of Environmental Science and Technology, Dalian University of Technology, Dalian 116024, China;* [‡]*Department of Chemical and Environmental Engineering, University of California, Riverside, California 92521, United States*

Abstract

Detection of highly toxic Cr(VI) is greatly desired. In the present study, a highly sensitive method for Cr(VI) detection by reduced graphene oxide (rGO) chemiresistor and 1,4-dithiothreitol (DTT) functionalized Au nanoparticles (AuNPs) is reported. The detection strategy is based on the selective binding between DTT functionalized AuNPs1 located in rGO conductive channels and DTT functionalized AuNPs2 in solution through the formation of disulfides induced by Cr(VI) at acidic condition, which results in aggregation of DTT functionalized AuNPs2 on the rGO channels producing a readily measurable resistance change. The response of the chemiresistor is rapid and allows real-time monitoring of Cr(VI). Using this method, as low as 0.9 nM of Cr(VI) in water was detected with good selectivity. The proposed method has great potentials for monitoring of trace Cr(VI) in drinking water.

Keywords: Cr(VI), Au nanoparticles, reduced graphene oxide, chemiresistor, electrical detection

1. Introduction

Expanded applications of chromium in industries, such as stainless steel manufacture, chrome-plating, leather tanning, and pigment production, result in the increasing leakage risk of dissolved chromium species including trivalent chromium (Cr(III)) and hexavalent chromium (Cr(VI)) into water. Unlike Cr(III), an essential element state for normal functioning of the human body [1], Cr(VI) is highly carcinogenic, and can induce DNA damage, gene mutations, and chromosomal aberrations [2, 3]. The U.S. Environmental Protection Agency (EPA) has set the maximum contaminant level (MCL) for total chromium in drinking water at 100 ppb. Thus, monitoring of trace Cr(VI) in water is critical to prevent potential chromium poisoning.

The traditional methods for detection of Cr(VI) include atomic absorption spectrometry, inductively coupled plasma-atomic emission spectrometry, inductively coupled plasma-mass spectrometry, and spectrophotometry [4-7]. These methods have several obvious shortcomings, such as needing expensive instruments, long analysis time due to complicated pretreatment procedures, or not enough sensitivity. Alternatively, several fast detection methods have been developed for the detection of Cr(VI), including electrochemical [1, 8], fluorescent [9], colorimetric [10], and surface-enhanced Raman scattering [11], with micromolar or nanomolar sensitivity. Despite these advancements, novel detection methods with simple operation, low cost, fast response, high sensitivity, and reliability are greatly needed.

In recent years, carbon nanomaterials-based field-effect transistor (FET) and chemiresistor have attracted increasing use as transducers combined with sensing

elements for highly selective and sensitive, real-time response, and label-free detection capabilities [12-14]. Graphene, a two-dimensional carbon nanomaterial with single atom thickness, not only has excellent electron mobility, thermal conductivity, mechanical strength, and large surface-to-volume ratio, but also shows unique tunable ambipolar characteristics and extremely low thermal and electrical noise due to high conductivity and few surface defects. Additionally, graphene overcomes the limitation of almost inevitable metallic impurities present in carbon nanotubes, which compromises the response performance in sensing platforms [15]. These merits have made graphene an attractive channel material of FET/chemiresistor and also sensing element for the detection of various analytes [16-18].

Au nanoparticles (AuNPs) are usually used to immobilize recognition probes containing thiol, such as DNA-SH, glutathione, etc., on graphene/carbon nanotube in many sensing devices due to extreme affinity between Au and –SH [10, 19, 20]. The immobilization could greatly improve sensitivity and dynamic range in FETs due to higher probe density compared with other immobilization methods [10]. On the other hand, Dong et al. used DNA labelled with AuNPs as a reporter probe for detection of DNA, achieving a significant sensitivity enhancement [21]. Park et al. reported a highly sensitive detection method for DNA by the selective binding between the DNA capture probe located in electrodes gap and DNA-functionalized AuNPs in solution [22]. These results showed great advantages for using AuNPs to improve the sensors response.

Recently, we reported a colorimetric assay (100 nM limit of detection) for Cr(VI) based on the change of color of DTT functionalized AuNPs in solution from red to purple as a result of aggregation induced by Cr(VI) at acidic condition [23]. In the present study, we further develop a sensor using reduced graphene oxide (rGO) chemiresistor with DTT functionalized

AuNPs as a recognition element for the detection of Cr(VI). The present sensor exhibited at least 100 times lower limit of detection for Cr(VI) than the colorimetric technique with a response time of approximately 50 s and good selectivity against commonly found cations in water.

2. Experimental

2.1 Material

Chloroauric acid ($HAuCl_4 \cdot 4H_2O$) was purchased from Shanghai Chemical Reagent Co. Ltd (Shanghai, China). 1-Pyrenemethylamine, 3-aminopropyltriethoxy silane, and sodium 2-mercaptoethanesulfonate were purchased from Sigma-Aldrich (USA). DTT (Biotechnology grade) was purchased from Jingkehongda Biotechnology Corp. (Beijing, China). Milli-Q® ultrapure water (18.2 MΩ) was used in all experiments. GO powder was purchased from Nanjing XFNANO Materials Tech. Co. Ltd (Nanjing, China). 0.5 mg/mL GO suspension was prepared by sonication at 250 W for 2 h using GO powder, followed by centrifugation at 300 g for 2 h with an Anke TGL-16G centrifuge (Shanghai, China). The supernatant was collected and centrifuged at 2200 g for 2 h. The pellet was collected and redispersed in DI water to form a uniform suspension with a concentration of ~50 μg/mL, measured by a colorimetric method referring to a known concentration GO suspension.

2.2 Fabrication of electrochemically derived rGO chemiresistor

Sensing devices were microfabricated on a SiO_2/Si wafer according to our previous report [24]. Each device contained five Au interdigitated electrode units, and each interdigitated electrode unit consisted of ten pairs of 200 μm long Au fingers separated by a 3 μm gap, as source and drain electrodes. The device was cleaned sequentially with acetone and piranha solution (a mixture of H_2SO_4 and 30% H_2O_2 (3:1 v/v), highly corrosive) followed by DI water and drying with N_2 after each step, and then incubated

with 3-aminopropyltriethoxy silane for 30 min after which the device was rapidly washed with plenty of DI water and dried with N_2. Five μL of GO suspension (50 μg/mL) was casted onto the fingers of the interdigitated electrode for 1 h, which was kept in a high humidity container to prevent drying of the GO suspension, followed by washing with DI water. The assembled GO sheets on the interdigitated electrode were reduced by a CHI 660D electrochemical workstation (Shanghai Chenhua, China) with a standard three electrodes system, where the interdigitated electrode was used as a working electrode, a Pt wire as a counter electrode, and an Ag/AgCl as a reference electrode. The electrochemical reduction was carried out in 100 mM PB (pH 7.4) by repeatedly sweeping the potential from 0 V to -1.5 V at a scan rate of 100 mV/s. The electrochemically reduced GO was annealed at 150 ^{o}C for 1 h in ambient air and was characterized by Raman spectroscopy (Fig. S1). The significant increase of the ID/IG ratio showed the successful reduction of GO [25].

2.3 Preparation and functionalization of AuNPs

Two different diameters AuNPs1 and AuNPs2 were prepared by the reduction of chloroauric acid with sodium borohydride and trisodium citrate as reducing agent, respectively, according to previous methods [23, 26]. The average diameters of AuNPs1 and AuNPs2 were ~6.5 nm and ~20 nm, respectively (Fig. S2 and S3). DTT functionalized AuNPs2 (DTT-AuNPs2) was prepared by mixing 1 mL AuNPs2 (1.5 nM) with 10 μL of 10 mM DTT and 10 μL of 20 mM 2-mercaptoethanesulfonate (prepared in deionized water deoxygenated by bubbling nitrogen for 30 min). After incubation for 1 h, the mixture was centrifuged at 10000 rpm for 30 min. The red precipitate was washed, recentrifuged, and finally dispersed in 1 mL sulfuric acid solution (1.5 mM, pH 2.5).

2.4 Assembly of AuNPs1 on rGO conductive channel

The interdigitated electrode with the electrochemically derived rGO was incubated with 8 mg/mL mPEG-SH (Mr = 350 Da) for 1 h to passivate bare Au fingers, followed by incubation with 1 mg/mL 1-pyrenemethylamine in dry dimethylformamide for 30 min, washed with dimethylformamide and 10 mM PB (pH 7.4). Then the interdigitated electrode was incubated with AuNPs1 for 1 h, which led to adsorption of AuNPs1 on the rGO conductive channel by electrostatic interaction. The resulting rGO with AuNPs1 was further incubated with 2 mM DTT solution for 1 h to obtain rGO with DTT-AuNPs1 channel, followed by washing with DI water.

2.5 Characterization

Morphological characterization of sensing channels was performed with a FEI nanoSEM 450 SEM (Eindhoven, The Netherlands). Raman spectra of rGO were obtained by a DXR Raman spectrometer (Thermo Fisher Scientific, USA) with an excitation wavelength of 532 nm. Transmission electron microscope (TEM) images of AuNPs were obtained by a FEI Tecnai G2 20. Size distribution and Zeta potentials of AuNPs were analyzed by a Malvern Zetasizer nano-ZS90 (Worcestershire, UK).

2.6 Sensing procedures

For the electrical measurement, a 200 μL volume PDMS chamber was attached onto the rGO with DTT-AuNPs1 sensing channels. The channels were exposed to 100 μL DTT-AuNPs2 (1.5 nM) in 1.5 mM sulfuric acid solution (pH 2.5) until the resistances in the channels were stable, followed by addition of 10 μL Cr(VI) (prepared in DI water) into the chamber. The drain current (I_{ds}) versus drain voltage (V_{ds}) or I_{ds} versus time (t) at a fixed V_{ds} were obtained by a Keithley 2602B digital source meter (Shanghai, China).

3. Results and Discussion

To construct the chemiresistor, GO was casted onto the interdigitated electrode, followed by the electrochemical reduction. The reduced GO was used as conductive channels between

Au fingers of the interdigitated electrode in the chemiresistor. The rGO channels were functionalized with 1-pyrenemethylamine, followed by adsorption of small diameter AuNPs1 (~6.5 nm) through electrostatic interaction, and then modification with DTT. The Au fingers were passivated with mPEG-SH to prevent affinity binding of DTT and DTT-AuNPs2 in solution. Each step of the rGO channels modification was confirmed by monitoring the change of the resistances in the channels based on the I_{ds}-V_{ds} curves (Fig. S4).

A high resolution SEM was used to characterize the distribution of AuNPs1 on the rGO channel. As shown in Fig. 1a, a few large nanoparticles, derived from aggregation of adjacent AuNPs1, were observed; however, monodisperse AuNPs1 couldn't be found due to poor image at high magnification. On the other hand, Energy-dispersive X-ray analysis showed that there was a high content (9.84%) of Au on the rGO channels (total content of C, O, Si, and Au was 100%) (Fig. S5). In order to obtain high quality SEM images of AuNPs1, large diameter AuNPs2 (~20 nm) were directly deposited on the rGO channels to increase their conductivity. In this case, AuNPs1 on the rGO channels were clearly observed, with a high density and more uniform distribution compared with the AuNPs2 (Fig. 1b). Further modification with DTT didn't lead to additional measurable change in the distribution of AuNPs1.

Fig. 2 shows the detection strategy of Cr(VI) with the rGO chemiresistor in conjunction with DTT functionalized AuNPs. When the rGO with DTT-AuNPs1 channel is exposed to only DTT-AuNPs2 or Cr(VI) solutions, the channel don't undergo any change and thus no response is produced. However, when the channel is exposed simultaneously to DTT-AuNPs2 and 0.5 μM Cr(VI) solutions, DTT-AuNPs2 aggregate on the rGO channel due to the selective binding between DTT-AuNPs1 located in the rGO channel and DTT-AuNPs2 in solution through the formation of disulfide bond (S-S). The aggregated DTT-AuNPs2 fill the electrodes gap and then improve the electron transfer, resulting in an increase of the

conductivity of the rGO channel.

The interaction between Cr(VI) and thiol species, such as cysteine and glutathione, has been extensively studied in the past decades.[27, 29-31]. At acidic condition, Cr(VI) is present mainly in $Cr_2O_7^{2-}$ form with strong oxidation ability. Generally, the formation of Cr(VI)-thioester intermediate with a large formation constant (1.4×10^3 M^{-1} at 25^oC) was considered to be an initial step, followed by subsequent electron transition to form Cr(Ⅲ) and oxidized thiol species [27]. Hence, the selective binding between DTT-AuNPs1 located in the rGO channel and DTT-AuNPs2 in solution in presence of Cr(VI) should be attributed to similar reaction processes, i.e. Cr(VI)-DTT-AuNPs intermediates were firstly formed, followed by the formation of disulfides between DTT-AuNPs1 and DTT-AuNPs2, leading to the aggregation of DTT-AuNPs2 on the rGO channel.

To prove that the electrical response of the rGO chemiresistor with DTT-AuNP1 was induced by Cr(VI), the rGO with DTT-AuNPs1 channel was exposed to DTT-AuNPs2 solution in absence and presence of Cr(VI). As shown in Fig.3, there was almost no change in the resistance of the channel when it was exposed to DTT-AuNPs2 solution in absence of Cr(VI). On the other hand, when 10 nM Cr(VI) was further added into the DTT-AuNPs2 solution, there was a 5.8% decrease of the resistance compared with the original resistance. Further, in addition of 200 nM Cr(VI), the channel produced a 17.8% decrease in the resistance. In fact, the response could also be observed using DTT-AuNPs1 instead of DTT-AuNPs2 in the solution, but a lower signal was achieved by the measurement. Therefore, DTT-AuNPs2 with large diameter was used to obtain higher sensitivity in following experiments.

Three comparison experiments were carried out to explore the role of DTT-AuNPs1 and DTT-AuNPs2 in the detection of Cr(VI) by the rGO chemiresistor. In the first experiment

rGO with DTT-AuNPs1 channel was exposed to Cr(VI) in absence of DTT-AuNPs2. As shown in Fig. 4, a small response (circle) was observed, which should be attributed to the direct interaction between Cr(VI) and DTT-AuNPs1 [27]. In the second test the rGO without DTT-AuNPs1 channel was incubated with DTT-AuNPs2 and Cr(VI). A larger response (triangle) was obtained compared with the first, which is ascribed to aggregation of DTT-AuNPs2 in the solution induced by Cr(VI) due to insufficient electrostatic repulsion between DTT-AuNPs2 with negative charges. In comparison, when the rGO with DTT-AuNPs1 channel was incubated simultaneously with DTT-AuNPs2 and Cr(VI), the sensor gave the most response (star).

From the above results, we can conclude: (1) Cr(VI) played a critical role in inducing the binding between DTT-AuNPs1 located in the rGO channel and DTT-AuNPs2 in solution and the response signal being the basis for the detection of Cr(VI); (2) a higher Cr(VI) detection sensitivity was obtained by the simultaneous use of DTT-AuNPs1 and DTT-AuNPs2 compared to using only DTT-AuNPs1 or DTT-AuNPs2; (3) the increased resistance change response with the concentration validated the potential of the rGO chemiresistor for quantitative measurement of Cr(VI) concentration in water.

As an additional confirmation of the Cr(VI) induced aggregation of DTT-AuNPs2 on the rGO with DTT-AuNPs1 channels, SEM images of the rGO channels before and after exposure to DTT-AuNPs2 in absence and presence of Cr(VI) were obtained. As shown in Fig. 5a and 5b, when the channels were incubated with DTT-AuNPs2 for 10 min, no DTT-AuNPs2 were observed on the rGO channels (Fig. 5a), indicating there was no binding between DTT-AuNPs1 located in the rGO channel and DTT-AuNPs2 in solution. However, when 0.5 μM Cr(VI) was further added, a great deal of DTT-AuNPs2 aggregated on the channels (Fig. 5b). EDX analysis showed that the

content of Au on the rGO channels increased from 9.84% following AuNPs1 adsorption to 11.95 % after aggregation of DTT-AuNPs2 in presence of Cr(VI). These findings confirmed that Cr(VI) induced the aggregation of DTT-AuNPs2 on the rGO channels through the selective binding to DTT-AuNPs1.

In the previous colorimetric analysis with DTT functionalized AuNPs, the optimized response was obtained at pH value ranging from 2.3~2.7. Here, similar results were obtained, i.e. DTT-AuNPs2 formed aggregates even in absence of Cr(VI) at pH below 2.3 producing a large background signal, whereas the sensor gave low sensitivity at pH over 2.7. Therefore, the solution was kept at pH 2.5 with 1.5 mM sulfuric acid solution for the detection of Cr(VI) in water. Salt could induce aggregation of AuNPs due to screening effect [28]. We found that DTT-AuNPs2 suspension was stable for 2 h when the salt (NaCl) concentration was less than 5 mM. Considering ~10 fold dilution of the sample in the sensing procedures, the present sensor could allow the maximum concentration of 50 mM for salt in the original water sample, which is higher than found in common clean water. Although temperature could accelerate the binding between DTT-AuNPs1 and DTT-AuNPs2 in presence of Cr(VI), DTT-AuNPs2 became unstable above 40 oC, resulting in a high background signal. Therefore, all measurements were performed at room temperature.

Fig. 6 shows the real-time response of the rGO with DTT-AuNPs1 channels incubated with DTT-AuNPs2 at a fixed source-drain voltage (V_{ds} = 0.1 V) upon addition of DI water and different concentration Cr(VI). While there was no change in the current (Ids) after addition of DI water, the sensor produced definitive increase of the I_{ds} upon exposure to as low as 0.9 nM Cr(VI), indicating that the addition of Cr(VI) resulted in an increase of the conductance of the rGO channels. Further, the response signal increased with the increase of Cr(VI) concentration. There was a good linear relationship between the response ($(I-I_0)/I_0$) and logarithmic value of Cr(VI) concentration ($y = 0.0233\ln(x) + 0.0361$, $R^2 = 0.996$). The lowest

concentration detected was 0.9 nM, which was at least three orders of magnitude lower than the MCL (~1.9 μM) enforced by the U.S. EPA for total chromium in drinking water. [18] Even considering that the sample added in the cell was diluted ~10-fold, the response signal was sufficient to detect MCL Cr(VI) levels in drinking water. Moreover, the sensor had a fast response time (~50 s) and is attributed to a rapid binding between DTT-AuNPs1 and DTT-AuNPs2 induced by Cr(VI) at acid condition.

Table 1 compares the analytical performance of the present rGO chemiresistive sensor to other methods for the detection of Cr(VI). The 0.9 nM LOD of the present sensor was superior than the lowest LOD reported for fluorescence (9.6 nM), colorimetric (1 nM), luminescence (24 nM), SERS (600 nM), SPRLS (20 nM), CV (30 nM), DPV (40 nM), impedimetric (30 nM), amperometric (3.8 nM), and potentiometric (63 nM) methods but higher than that of SSWV (0.06 nM), ASV (0.09 nM), and photoelectrochemical (0.1 nM) detection methods. The improved LOD for ASV, SSWV, and the photoelectrochemical methods can be attributed to the use of an accumulation step to enrich Cr(VI) in sample solution prior to the detection and increasing the incubation time could efficiently enhance the detection sensitivity of the present sensor. Compared with ASV and SSWV, the present sensor has advantages of 1) a short response time (less than 50 s compared to 20 to 300 s) and thus allowing a real-time monitoring and 2) a wider dynamic range (0.9 to 800 nM compared to 0.5 to 50 nM) for the quantification of Cr(VI). Further, the sensor has a higher sensitivity compared to the traditional detection methods of AAS, ICP-AES, ICP-MS, and spectrophotometry.

To investigate the rGO chemiresistive sensor specificity, the sensor response to Cr(VI) was compared to that for other common metal ions found in water at identical concentrations (100 nM). The current (Ids) was monitored when different metal ions (Na^+, K^+, Ca^{2+}, Ni^{2+}, Zn^{2+}, Pb^{2+}, Al^{3+}, Fe^{3+}, Cr^{3+}, Mn^{2+}, and Hg^{2+}) were added to the

solution chamber, respectively. As shown in Fig. 7, the sensor showed very low to no responses to Na^+, K^+, Ca^{2+}, Ni^{2+}, Zn^{2+} and Pb^{2+} ions, since these ions didn't induce the binding between DTT-AuNPs1 and DTT-AuNPs2. Al^{3+} and Fe^{3+}, however, produced a small response. The response to Fe^{3+} may be attributed to its' oxidation action, resulting in the binding between DTT-AuNPs1 and DTT-AuNPs2, similar to that induced by Cr(VI). The response to Al^{3+} can be ascribed to the binding between Al^{3+}, a strong Lewis acid, and –SH, a strong Lewis base. Cr^{3+} with same charges as Al^{3+} and Fe^{3+} produced a very small response due to the weak interaction between Cr^{3+} and –SH. The sensor shows an obvious response to Hg^{2+}, which was attributed to the high affinity between Hg^{2+} and –SH. The response to Mn^{2+} is presently not understood and further study is needed to comprehend the principle. In general, the present method for Cr(VI) is competent for relatively clean water samples such as drinking water and is not suitable for wastewater due to potential interferes of other metal ions such as Al^{3+}, Fe^{3+}, Mn^{2+}, and Hg^{2+}.

The reproducibility of the sensor was evaluated. Three sensing devices were prepared in different batches (each device contained five same sensing channels, i.e. sensors) to detect Cr(VI) of 10 nM and 200 nM standard solutions. The RSDs of five sensors within one device were 9.2% and 6.8% while the RSDs between the devices, i.e. batch to batch variability, was 15.2% and 12.6% for the samples, respectively. These results showed that the present sensing devices could be fabricated repeatedly by the described protocol.

To evaluate the applicability of the present method for practical application, the sensor was applied to detect Cr(VI) concentration of local tap and reservoir water . The initial detection showed no presence of chromium including Cr(III) and Cr(VI) in the samples with ICP-AES (PerkinElmer Optima 2000DV). Cr(VI) standard solution

was spiked in the samples with the final concentrations of 10 nM and 200 nM, and then detected by the sensor with the sensing procedures. The recoveries ranged from 95.3~126.0% and the RSDs ranged from 5.4% to 14.6% (Table 2). A relatively high recovery for the tap water sample spiked with 10 nM Cr(VI) might be ascribed to the interference of Fe^{3+} from release from the iron water pipe.

To further investigate if the sensor responded to other oxidizers, we checked the response of the present sensor to H_2O_2, which is a stronger oxidizer than Cr(VI) based on the redox potentials (1.77 V versus 1.33 V). As shown in Fig. 8, the sensor elicited an obvious response only above 7 μM H_2O_2 concentration and the sensitivity was at least 100 times lower than that for Cr(VI). Colorimetric analysis with DTT-AuNPs2 gave similar results, i.e. lower sensitivity for H_2O_2 than for Cr(VI) (Fig. S6). This finding indicated that the Cr(VI)- DTT functionalized AuNPs intermediate played an important role in the sensitive detection of Cr(VI) by the rGO chemiresistor using DTT functionalized AuNPs.

4. Conclusions

We have fabricated a rGO chemiresistive sensor by using DTT functionalized AuNPs as recognition element for highly sensitive detection of Cr(VI) in drinking water. The detection is based on the selective binding between DTT-AuNPs1 located in rGO conductive channel and DTT-AuNPs2 in solution in presence of Cr(VI), which results in aggregation of DTT-AuNPs2 on the rGO channel leading to a measurable resistance change. The present sensor shows fast response and allows it to carry out real-time monitoring of Cr(VI). The lowest detected concentration is 0.9 nM. The proposed platform has a great potential for monitoring trace Cr(VI) in environmental water samples. We are exploring a similar strategy to detect Hg^{2+} ion by using two complementary DNAs with T–T mismatches for functionalization of AuNPs1 and

AuNPs2, respectively. Because of high specificity of T–Hg^{2+}–T coordination, [32, 33] the Hg^{2+} sensor will have a high sensitivity and selectivity.

Acknowledgements

We acknowledge the financial support of the Basic Research Program of Key Laboratory, Education Department of Liaoning Province, China (No. LZ2014008), the 111 Project (B13012), the National Science Foundation, U.S. Department of Agriculture and W. Ruel Johnson Chair in Environmental Engineering.

References

1 J. Wei, Z. Guo, X. Chen, D.-D. Han, X.-K. Wang, X.-J. Huang, Ultrasensitive and ultraselective impedimetric detection of Cr(VI) using crown ethers as high-affinity targeting receptors, Anal. Chem., 87(2015) 1991-1998.

2 A.M. Urbano, C.F.D. Rodrigues, M.C. Alpoim, Hexavalent chromium exposure, genomic instability and lung cancer, Gene Ther. Mol. Biol., 12B(2008) 219-238.

3 S. Majumder, K. Ghoshal, D. Summers, S.M. Bai, J. Datta, S.T. Jacob, Chromium(VI) down-regulates heavy metal-induced metallothionein gene transcription by modifying transactivation potential of the key transcription factor, metal-responsive transcription factor 1, J. Biol. Chem., 278(2003) 26216-26226.

4 I. Lopez-Garcia, Y. Vicente-Martinez, M. Hernandez-Cordoba, Determination of very low amounts of chromium(III) and (VI) using dispersive liquid-liquid microextraction by in situ formation of an ionic liquid followed by electrothermal atomic absorption spectrometry, J. Anal. At. Spectrom., 27(2012) 874-880.

5 T. Sumida, T. Ikenoue, K. Hamada, A. Sabarudin, M. Oshima, S. Motomizu, On-line preconcentration using dual mini-columns for the speciation of chromium(III) and chromium(VI) and its application to water samples as studied by inductively coupled plasma-atomic emission spectrometry, Talanta, 68(2005) 388-393.

6 Y. Martinez-Bravo, A.F. Roig-Navarro, F.J. Lopez, F. Hernandez, Multielemental determination of arsenic, selenium and chromium(VI) species in water by high-performance liquid chromatography-inductively coupled plasma mass spectrometry, J. Chromatogr. A, 926(2001) 265-274.

7 M.S. El-Shahawi, S.S.M. Hassan, A.M. Othman, M.A. Zyada, M.A. El-Sonbati, Chemical speciation of chromium(III,VI) employing extractive spectrophotometry and tetraphenylarsonium chloride or tetraphenylphosphonium bromide as ion-pair reagent, Anal. Chim. Acta, 534(2005) 319-326.

8 L.E. Korshoj, A.J. Zaitouna, R.Y. Lai, Methylene blue-mediated electrocatalytic detection of hexavalent chromium, Anal. Chem., 87(2015) 2560-2564.

9 S.J. Toal, K.A. Jones, D. Magde, W.C. Trogler, Luminescent silole nanoparticles as chemoselective sensors for Cr(VI), J. Am. Chem. Soc., 127(2005) 11661-11665.

10 W. Chen, F. Cao, W. Zheng, Y. Tian, Y. Xianyu, P. Xu, et al., Detection of the nanomolar level of total Cr (III) and (VI) by functionalized gold nanoparticles and a smartphone with the assistance of theoretical calculation models, Nanoscale, 7(2015) 2042-2049.

11 Y. Ye, H. Liu, L. Yang, J. Liu, Sensitive and selective SERS probe for trivalent chromium detection using citrate attached gold nanoparticles, Nanoscale, 4(2012) 6442-6448.

12 R. Stine, J.T. Robinson, P.E. Sheehan, C.R. Tamanaha, Real-time DNA detection using reduced graphene oxide field effect transistors, Adv. Mater., 22(2010) 5297-5300.

13 E. Stern, A. Vacic, N.K. Rajan, J.M. Criscione, J. Park, B.R. Ilic, et al., Label-free biomarker detection from whole blood, Nat. Nanotechnol., 5(2010) 138-142.

14 B. Cai, S. Wang, L. Huang, Y. Ning, Z. Zhang, G.-J. Zhang, Ultrasensitive label-free detection of PNA-DNA hybridization by reduced graphene oxide field-effect transistor biosensor, ACS Nano, 8(2014) 2632-2638.

15 W.R. Yang, K.R. Ratinac, S.P. Ringer, P. Thordarson, J.J. Gooding, F. Braet, Carbon nanomaterials in biosensors: should you use nanotubes or graphene?, Angew. Chem. Int. Ed., 49(2010) 2114-2138.

16 B.B. Zhan, C. Li, J. Yang, G. Jenkins, W. Huang, X.C. Dong, Graphene field-effect transistor and its application for electronic sensing, Small, 10(2014) 4042-4065.

17 R. Stine, S.P. Mulvaney, J.T. Robinson, C.R. Tamanaha, P.E. Sheehan, Fabrication, optimization, and use of graphene field effect sensors, Anal. Chem., 85(2013) 509-521.

18 C.Y. Wang, X.Y. Cui, Y. Li, H.B. Li, L. Huang, J. Bi, et al., A label-free and portable graphene FET aptasensor for children blood lead detection, Sci. Rep., 6(2016) 21711.

19 K.H. Chen, G.H. Lu, J.B. Chang, S. Mao, K.H. Yu, S.M. Cui, et al., Hg(II) ion detection using thermally reduced graphene oxide decorated with functionalized gold nanoparticles, Anal. Chem., 84(2012) 4057-4062.

20 G. Zhou, J. Chang, S. Cui, H. Pu, Z. Wen, J. Chen, Real-time, selective detection of pb2+ in water using a reduced graphene oxide/gold nanoparticle field-effect transistor device, ACS Appl. Mater. Interfaces, 6(2014) 19235-19241.

21 X.C. Dong, C.M. Lau, A. Lohani, S.G. Mhaisalkar, J. Kasim, Z.X. Shen, et al., Electrical detection of femtomolar DNA via gold-nanoparticle enhancement in carbon-nanotube-network field-effect transistors, Adv. Mater., 20(2008) 2389-2393.

22 P. So-Jung, T.A. Taton, C.A. Mirkin, Array-based electrical detection of DNA with nanoparticle probes, Science, 295(2002) 1503-1506.

23 F. Tan, X. Liu, X. Quan, J. Chen, X. Li, H. Zhao, Selective detection of nanomolar Cr(VI) in aqueous solution based on 1,4-dithiothreitol functionalized gold nanoparticles, Anal. Methods, 3(2011) 343-347.

24 F. Tan, N.M. Saucedo, P. Ramnani, A. Mulchandani, Label-free electrical immunosensor for highly sensitive and specific detection of microcystin-lr in water samples, Environ. Sci. Technol., 49(2015) 9256-9263.

25 S.T. Nguyen, R.S. Ruoff, S. Stankovich, D.A. Dikin, R.D. Piner, K.A. Kohlhaas, et al., Synthesis of graphene-based nanosheets via chemical reduction of exfoliated graphite oxide, Carbon, 45(2007) 1558-1565.

26 N.R. Jana, L. Gearheart, C.J. Murphy, Seeding growth for size control of 5-40 nm diameter gold nanoparticles, Langmuir, 17(2001) 6782-8786.

27 R.N. Bose, S. Moghaddas, E. Gelerinter, Long-lived chromium(IV) and chromium(V) metabolites in the chromium(VI) glutathione reaction: NMR, ESR, HPLC, and kinetic characterization, Inorg. Chem., 31(1992) 1987-1994.

28 C.W. Liu, Y.T. Hsieh, C.C. Huang, Z.H. Lin, H.T. Chang, Detection of mercury(II) based on Hg(2+)-DNA complexes inducing the aggregation of gold nanoparticles, Chem. Commun., (2008) 2242-2244.

29 E. Gaggelli, F. Berti, N. Gaggelli, A. Maccotta, G. Valensin, A homodinuclear Cr-v-Cr-v complex forms from the chromate-glutathione reaction in water, J. Am. Chem. Soc., 123(2001) 8858-8859.

30 A. Levina, P.A. Lay, Solution structures of chromium(VI) complexes with glutathione and model thiols, Inorg. Chem., 43(2004) 324-335.

31 P.A. Lay, A. Levina, Kinetics and mechanism of chromium(VI) reduction to chromium(III) by L-cysteine in neutral aqueous solutions, Inorg. Chem., 35(1996) 7709-7717.

32 J.-S. Lee, M.S. Han, C.A. Mirkin, Colorimetric detection of mercuric ion (Hg^{2+}) in aqueous media using DNA-functionalized gold nanoparticles, Angew. Chem. Int. Ed., 46(2007) 4093-4096.

33 B.C. Ye, B.C. Yin, Highly Sensitive Detection of Mercury(II) Ions by Fluorescence Polarization Enhanced by Gold Nanoparticles, Angew. Chem. Int. Ed., 47(2008) 8386-8389.

34 I. Ignatiadis, C. Michel, A. Ouerd, F. Battaglia-Brunet, N. Guigues, J.P. Grasa, et al., Cr(VI) quantification using an amperometric enzyme-based sensor: Interference and physical and chemical factors controlling the biosensor response in ground waters, Biosens. Bioelectron., 22(2006) 285-290.

35 W. Jin, G.S. Wu, A.C. Chen, Sensitive and selective electrochemical detection of chromium(VI) based on gold nanoparticle-decorated titania nanotube arrays, Analyst, 139(2014) 235-241.

36 B. Bas, Refreshable mercury film silver based electrode for determination of chromium(VI) using catalytic adsorptive stripping voltammetry, Anal. Chim. Acta, 570(2006) 195-201.

37 M. Grabarczyk, M. Korolczuk, L. Kaczmarek, Simple and highly selective catalytic adsorptive voltammetric method for Cr(VI) determination, Electroanalysis, 18(2006) 2381-2384.

38 R.Z. Ouyang, S.A. Bragg, J.Q. Chambers, Z.L. Xue, Flower-like self-assembly of gold nanoparticles for highly sensitive electrochemical detection of chromium(VI), Anal. Chim. Acta, 722(2012) 1-7.

39 O. Dominguez-Renedo, L. Ruiz-Espelt, N. Garcia-Astorgano, M.J. Arcos-Martinez, Electrochemical determination of chromium(VI) using metallic nanoparticle-modified carbon screen-printed electrodes, Talanta, 76(2008) 854-858.

40 R.A. Sanchez-Moreno, M.J. Gismera, M.T. Sevilla, J.R. Procopio, Evaluation of solid-state platforms for chromium (VI) potentiometric sensor development, Sens. Actuators, B, 143(2010) 716-723.

41 T. Fang, X.M. Yang, L.Z. Zhang, J.M. Gong, Ultrasensitive photoelectrochemical determination of chromium(VI) in water samples by ion-imprinted/formate anion-incorporated graphitic carbon nitride nanostructured hybrid, J. Hazard. Mater., 312(2016) 106-113.

42 F. Cai, X.D. Liu, S. Liu, H. Liu, Y.M. Huang, A simple one-pot synthesis of highly fluorescent nitrogen-doped graphene quantum dots for the detection of Cr(VI) in aqueous media, RSC Adv., 4(2014) 52016-52022.

43 H.Y. Zhang, Q. Liu, T. Wang, Z.J. Yun, G.L. Li, J.Y. Liu, et al., Facile preparation of glutathione-stabilized gold nanoclusters for selective determination of chromium (III) and chromium (VI) in environmental water samples, Anal. Chim. Acta, 770(2013) 140-146.

44 W. Ji, Y. Wang, I. Tanabe, X.X. Han, B. Zhao, Y. Ozaki, Semiconductor-driven "turn-off" surface-enhanced Raman scattering spectroscopy: application in selective determination of chromium(VI) in water, Chem. Sci., 6(2015) 342-348.

45 Z.Q. Han, L. Qi, G.Y. Shen, W. Liu, Y. Chen, Determination of chromium(VI) by surface plasmon field-enhanced resonance light scattering, Anal. Chem., 79(2007) 5862-5868.

46 A. Ravindran, M. Elavarasi, T.C. Prathna, A.M. Raichur, N. Chandrasekaran, A. Mukherjee, Selective colorimetric detection of nanomolar Cr (VI) in aqueous solutions using unmodified silver nanoparticles, Sens. Actuators, B, 166(2012) 365-371.

47 L. Fei-Ming, L. Jia-Ming, W. Xin-Xing, L. Li-Ping, C. Wen-Lian, L. Xuan, et al., Non-aggregation based label free colorimetric sensor for the detection of Cr (VI) based on selective etching of gold nanorods, Sens Actuators, B Chem, 155(2011) 817-822.

48 H.Q. Chen, J.C. Ren, Sensitive determination of chromium (VI) based on the inner filter effect of upconversion luminescent nanoparticles (NaYF4:Yb3+, Er3+), Talanta, 99(2012) 404-408.

49 M.L. Cui, G. Song, C. Wang, Q.J. Song, Synthesis of cysteine-functionalized water-soluble luminescent copper nanoclusters and their application to the determination of chromium(VI), Microchim. Acta, 182(2015) 1371-1317.

Table 1 Comparison between the rGO chemiresistor to other methods for the detection of Cr(VI)[a]

Detection method	Sensing/recognition material	Acc. time	Linear range (nM)	LOD (nM)	Ref.
Impedimetric	Crown ethers/Au electrode	1 h	19~1.9x10^3	30	[1]
Amperometric	Cr(VI)-reductase cytochrome c3	/	/	3.8	[34]
CV	Methylene blue/Au electrode	/	100~5 x10^4	100	[8]
CV	AuNPs/TiO2 nanotubes	/	100~1x10^5	30	[35]
ASV	Hg film/Ag electrode	20 s	0.5~50	0.19	[36]
ASV	HMDE	30 s	0.2~2	0.09	[37]
SSWV	AuNPs/GCE	300 s	0.19~23	0.06	[38]
DPV	AuNPs/SPCE	/	400~3x10^4	40	[39]
Potentiometric	Diphenylcarbazide/CPE	/	1x10^3~1 x10^4	63	[40]
PEC	graphitic carbon nitride	600 s	0.19~19	0.1	[41]
Fluorescence	N-doping GQD	/	0~1.4 x10^5	40	[42]
Fluorescence	glutathione-AuNPs nanoclusters	/	96~9.6 x10^3	9.6	[43]
SERS	alizarin red S-sensitized TiO_2NPs	/	600~1 x10^4	600	[44]
SPRLS	rhodamine B and KI	/	40~320	20	[45]
Colorimetric	AgNPs	/	1~1 x10^6	1	[46]
Colorimetric	Au nanorods	/	100~2 x10^4	88	[47]
Luminescence	NaYF4:Yb^{3+}, Er^{3+} nanoparticles	/	70~1 x10^4	24	[48]
Luminescence	Cu nanoclusters	/	200~6 x10^4	65	[49]
Chemiresistor	rGO with DTT-AuNPs	/	0.9~800	0.9	This work

[a]Abbreviations: adsorptive striping voltammetry (ASV); photoelectrochemical (PEC); glassy carbon electrode(GCE); square wave voltammetry (SWV); hanging mercury drop electrode (HMDE); carbon paste electrode (CPE); Graphene quantum dots(GQD); screen-printed carbon electrode (SPCE); differential pulse voltammetry (DPV); stripping square wave voltammetry (SSWV); surface plasmon resonance light scattering (SPRLS); surface-enhanced Raman scattering (SERS)

Table 2 Analytical results of spiked real water samples by the proposed method (n = 4~5).

Samples	Spiked (nM)	Found (nM)	Recovery (%)	RSD (%)	ICP-OES (nM)
Tap water	10	12.6	126.0%	9.8	9.8
	200	194.6	97.3%	7.4	197.4
Reservoir water	10	10.6	106.0%	14.6	10.2
	200	190.6	95.3%	5.4	198.6

Figures captions

Figure 1. SEM of rGO channel with AuNPs1 before (A) and after (B) deposition of AuNPs2

Figure 2. Schematic diagram of the detection strategy of Cr(VI) with the rGO chemiresistor by using DTT-AuNPs.

Figure 3. I_{ds}-V_{ds} curves of the rGO with DTT-AuNPs1 channels exposure to Cr(VI) in presence of DTT-AuNPs2 in 1.5 mM H_2SO_4 (pH 2.5). (1) Original, (2) DTT-AuNPs2, (3) DTT-AuNPs2 + 10 nM Cr(VI), (4) DTT-AuNPs2 + 200 nM Cr(VI).

Figure 4 Response of the rGO with DTT-AuNPs1 channel exposed to Cr(VI) (circle), rGO channel exposed to DTT-AuNPs2 and Cr(VI) (triangle), and rGO with DTT-AuNPs1 channel exposed to DTT-AuNPs2 and Cr(VI) (star). The data were average value of 4~5 sensing channels.

Figure 5 SEM of the rGO channels at different conditions. (A) rGO with DTT-AuNPs1 channels exposure to DTT-AuNPs2, (B) rGO with DTT-AuNPs1 channel exposure to DTT-AuNPs2 and 0.5 μM Cr(VI)

Figure 6 Real-time response of the sensor upon exposure to different Cr(VI) concentrations at fixed voltage (V_{ds} =0.1 V). The concentrations in figure are the cumulative concentrations after sequential addition of Cr(VI).

Figure 7 Real-time response of the sensor upon exposure to Cr(VI) and other metal ions (A) and relative current change of the sensor to 100 nM different metal ions (B). The concentrations labelled in figure are the cumulative concentrations after sequential addition of Cr(VI). V_{ds} = 0.1 V

Figure 8 Response of the present sensor to Cr(VI) (a) and H_2O_2 (b), (circle) Cr(VI), (square) H_2O_2

Figure 1

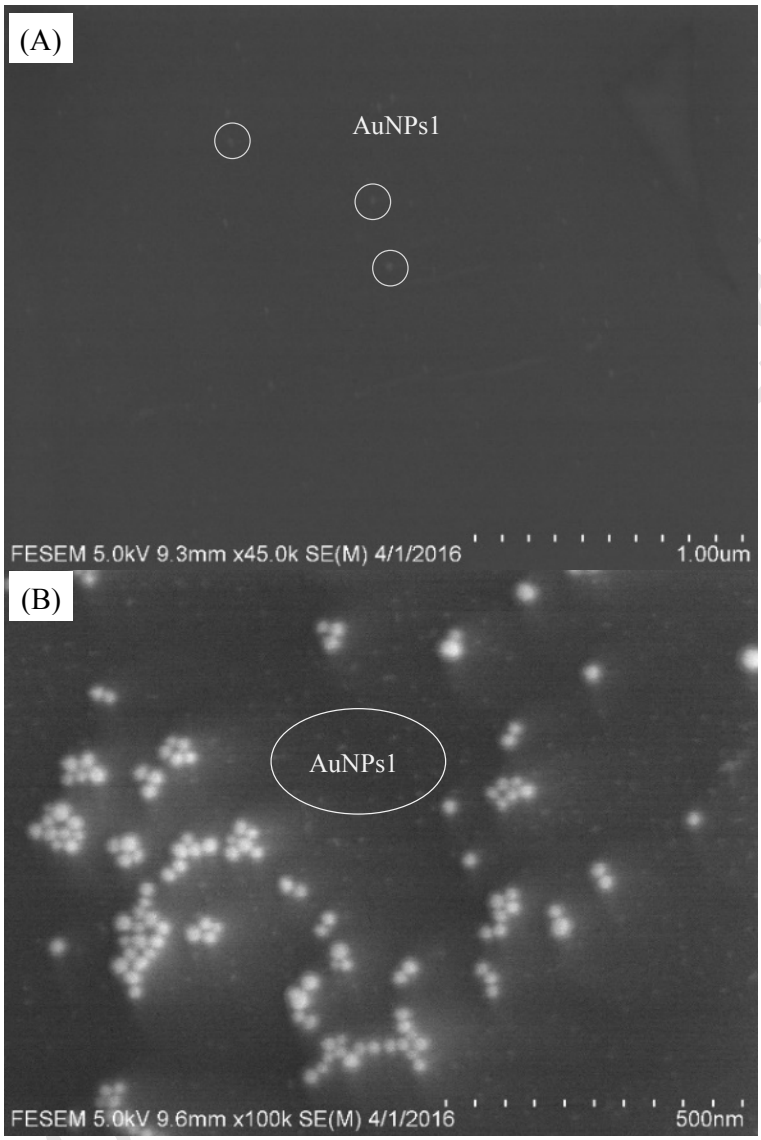

Figure 2

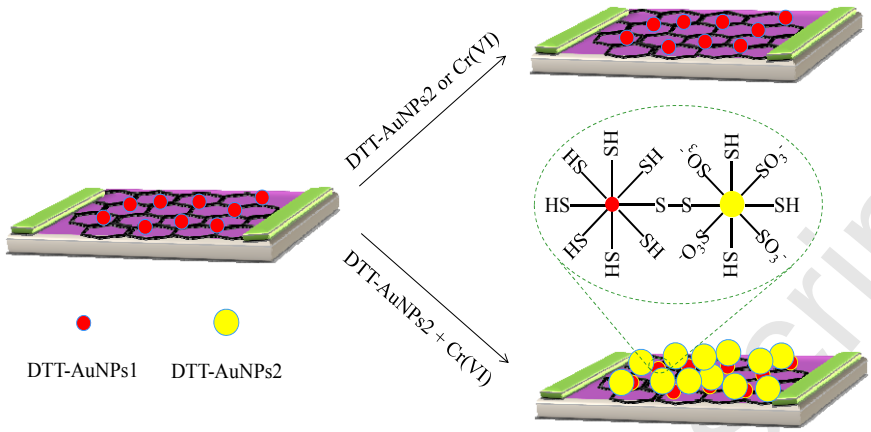

Figure 3

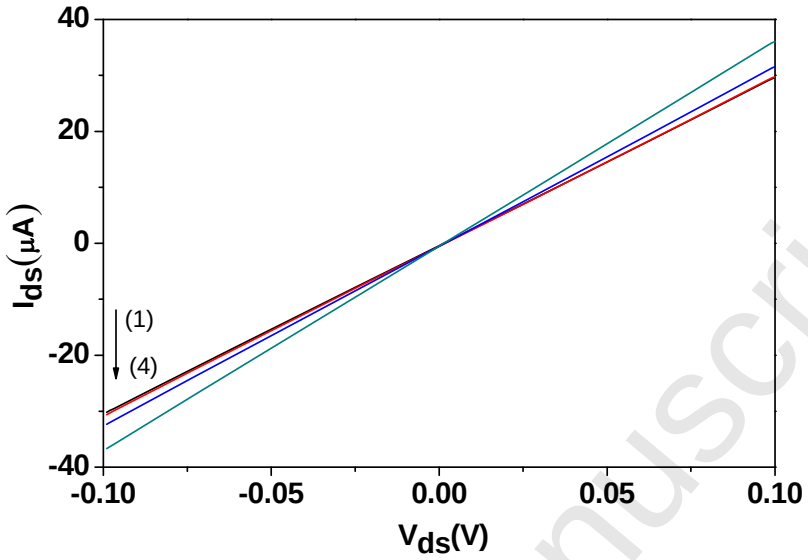

Figure 4

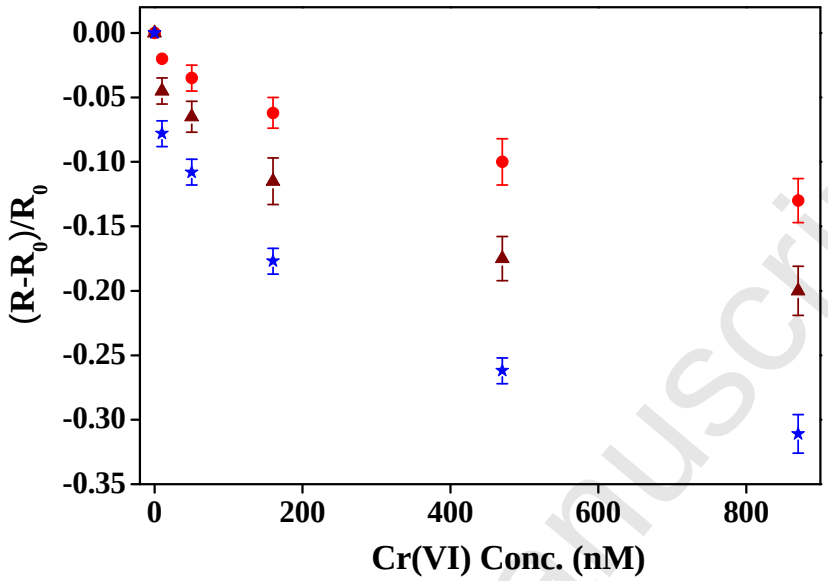

Figure 5

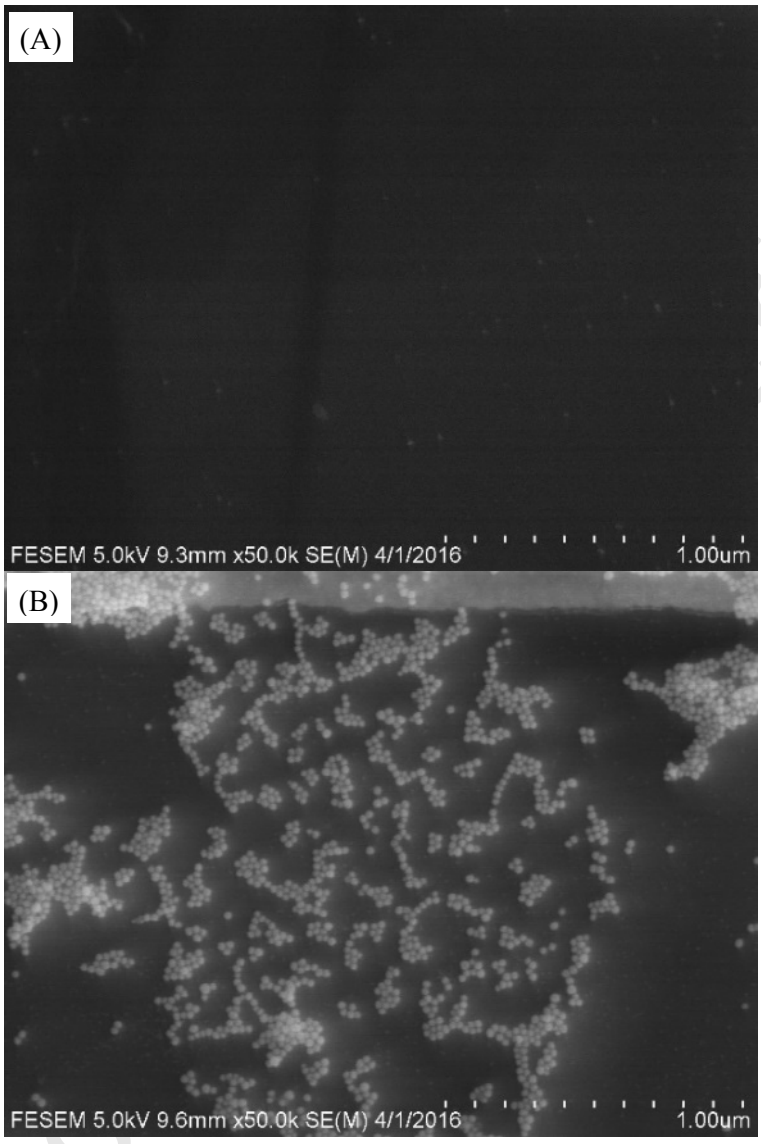

Figure 6

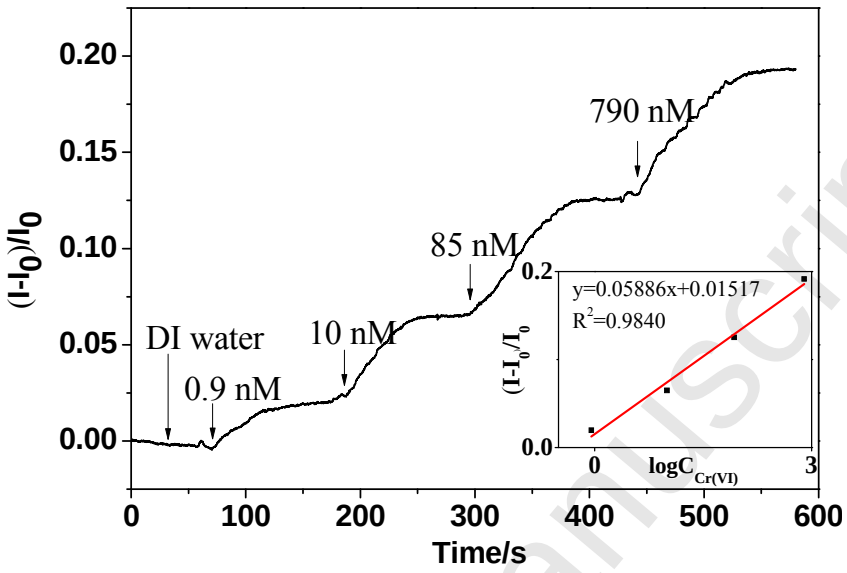

Figure 7

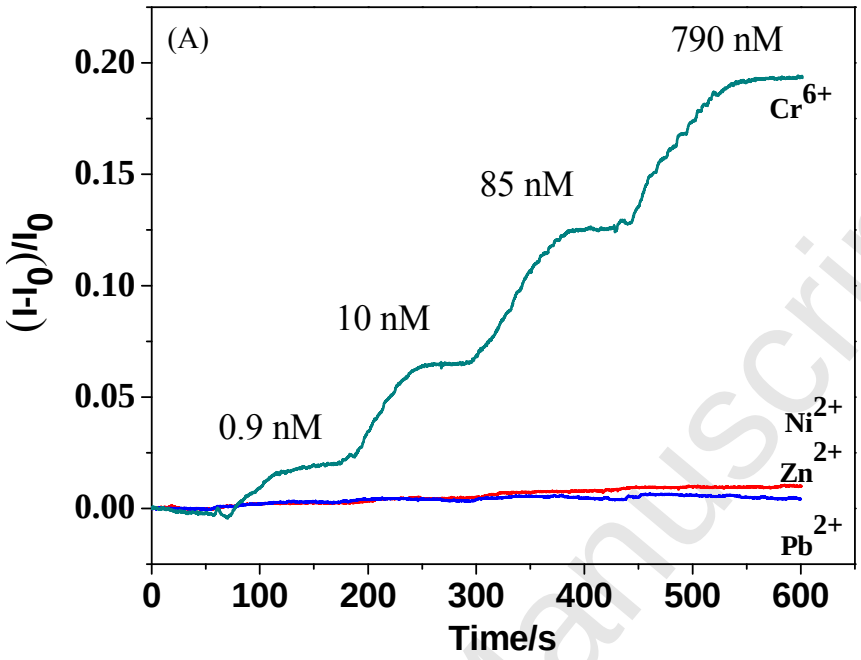

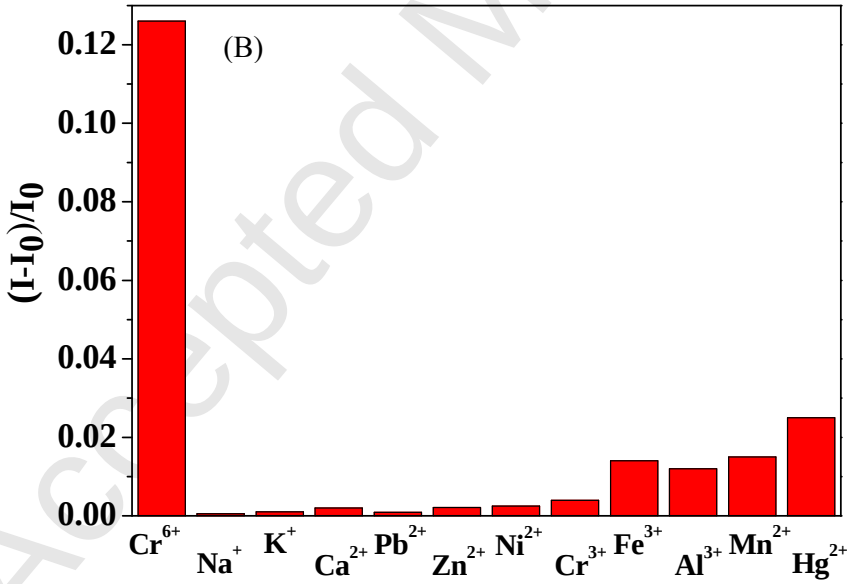

Figure 8

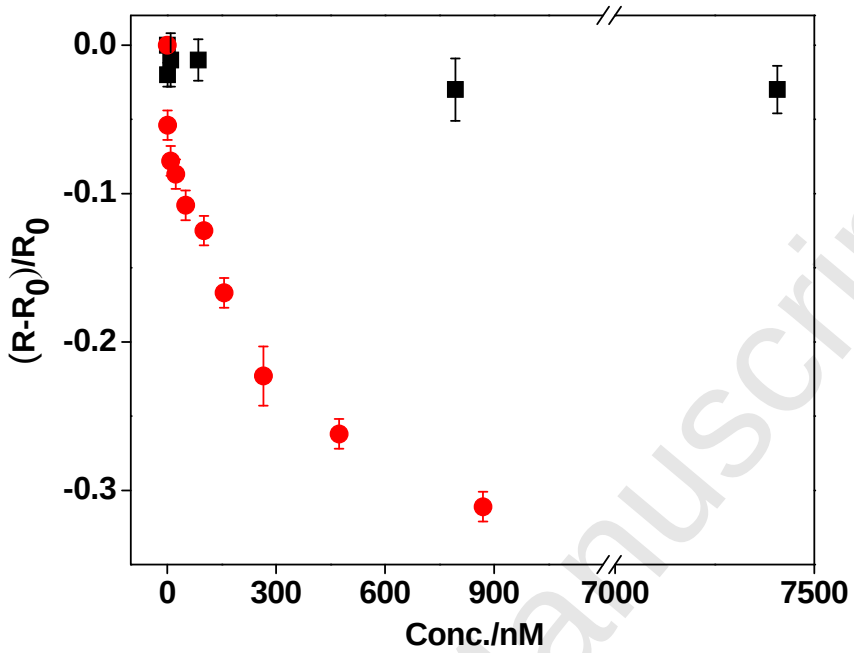

Biographies

Feng Tan received his PhD in Analytical Chemistry from Dalian Institute of Chemical Physics, Chinese Academy of Sciences in 2005. Now he is an associate professor at Dalian University of Technology, China. His researches focus on biosensors and functional nanomaterials for pollution control.

Longchao Cong is a M.S. candidate in Environmental Engineering at Dalian University of Technology, China. His current research focuses on biosensors.

Xiao Jiang is a M.S. candidate in Environmental Engineering at Dalian University of Technology, China. Her current research focuses on functional nanomaterials for analysis of environmental pollutants.

Yi Wang is a M.S. candidate in Environmental Engineering at Dalian University of Technology, China. His current research focus on electrochemical sensors

Xie Quan received his PhD in 2000 at University of Graz, Austria. In 1997. He was appointed a full professor in Dalian University of Technology, China. In 2005, he was appointed as Changjiang Scholar distinguished Professor by Chinese Ministry of Education and a winner of the National Science Fund for Distinguished Young Scholars. His interests include water pollution control, environmental monitoring, and environmental material applications.

Jingwen Chen received his PhD in Environmental Chemistry from Nanjing University, China in 1997. In 2001, he was promoted to be a full professor. In 2013, he was appointed as Changjiang Scholar distinguished Professor by Chinese Ministry of Education and a winner of the National Science Fund for Distinguished Young Scholars. His current interests include pollution eco-chemistry, computational and ecological toxicology.

Ashok Mulchandani is a professor in the Department of Chemical and Environmental Engineering at the University of California and the Editor-in-Chief of the Applied

Biochemistry and Biotechnology journal. He is elected Fellow of the American Association for Advancement of Science and the American Institute for Medical and Biological Engineering. He has received several honors and awards including Research Initiation Award from the National Science Foundation and Faculty Participation Award from the Department of Energy. He has delivered several Plenary and Keynote lectures. He has published over 250 peer-reviewed journal publications, 13 book chapters, 12 conference proceedings articles, over 200 conference abstracts and edited four textbooks. Prof. Mulchandani's primary research interest is in the broad area of "Bio-Nanotechnology" with goals of developing novel (bio)analytical devices/assays, (bio)remediation technologies and (bio)nanomaterials.